

Stop and sbottom LSP with R-parity violationEung Jin Chun,^{1,*} Sunghoon Jung,^{1,†} Hyun Min Lee,^{2,‡} and Seong Chan Park^{1,3,§}¹*Korea Institute for Advanced Study, Seoul 130-722, Korea*²*Department of Physics, Chung-Ang University, Seoul 156-756, Korea*³*Department of Physics, Sungkyunkwan University, Suwon 440-746, Korea*

(Received 20 November 2014; published 29 December 2014)

Considering a third-generation squark as the lightest supersymmetric particle (LSP), we investigate R-parity violating collider signatures with bilinear LH or trilinear LQD operators that may contribute to observed neutrino masses and mixings. Reinterpreting various LHC 7 + 8 TeV results of supersymmetry and leptoquark searches, we find that third-generation squark LSPs decaying to first- or second-generation leptons are generally excluded up to at least about 660 GeV at 95% C.L. One notable feature of sbottom LSP models, as opposed to stop LSP models, is that sbottoms can decay to top quarks leading to a broader invariant mass spectrum and weaker constraints in current collider searches. More dedicated searches with *b*-taggings or top reconstructions are thus encouraged. Finally, we discuss that the recently observed excesses in the CMS leptoquark search can be accommodated by decays of mostly left-handed sbottom LSPs in the LQD₁₁₃₊₁₃₁ model.

DOI: 10.1103/PhysRevD.90.115023

PACS numbers: 12.60.Jv, 14.60.Pq, 14.80.Ly

I. INTRODUCTION

Supersymmetry (SUSY) has been considered as a leading candidate for physics beyond the Standard Model because it provides a natural framework to stabilize the weak scale against huge quantum corrections. The CMS and ATLAS collaborations of the LHC experiment have been performing a broad range of searches for SUSY in various channels. After the LHC Run-1 with the $\sqrt{s} = 7, 8$ TeV collision energies, the first two generation squarks and gluinos are already excluded up to 1–2 TeV and the third-generation squarks up to 400–700 GeV depending on various search channels with R-parity conservation (RPC) or violation (RPV) [1]. Among three generations of squarks, the third-generation squarks are of particular interest, as they contribute significantly to the Higgs mass through loop corrections, and thus direct stop/sbottom searches at the LHC are motivated.

As is well known, the Standard Model gauge invariance allows bilinear (LH) and trilinear (LLE, LQD) lepton-number (*L*) violating operators as well as trilinear (UDD) baryon-number (*B*) violating operators in the renormalizable superpotential (each operator corresponds to each term below in order):

$$W_{\text{RPV}} = \epsilon_i \mu L_i H_u + \lambda_{ijk} L_i L_j E_k^c + \lambda'_{ijk} L_i Q_j D_k^c + \lambda''_{ijk} U_i^c D_j^c D_k^c, \quad (1)$$

where μ denotes the supersymmetric mass parameter of the Higgs bilinear operator $H_u H_d$. The simultaneous presence

of *L* and *B* violating terms makes protons unstable and thus has to be avoided. Proton stability may be ensured by imposing various discrete symmetries [2]. One of them is the standard R-parity [3] forbidding all of the above operators.¹ Other popular options are to consider the B-parity and L-parity, forbidding only *B* and *L* violating operators, respectively. The B-parity has an attractive feature that the allowed *L* violating operators could be the origin of tiny neutrino masses [4–6].

Motivated by these, we investigate signatures of the stop/sbottom LSP directly decaying into a quark and a lepton through either the bilinear LH or trilinear LQD couplings which can contribute to the observed neutrino masses and mixing. One of the search channels for such RPV stops/sbottoms is the conventional leptoquark search [7], which has been carried out at the HERA [8] and more recently at the LHC [9–12]. RPV signatures of the stop LSP were studied earlier in Refs. [13] and more recently in Ref. [14]. Leptoquark signatures of the stop/sbottom LSP have also been explored recently in Ref. [15] in the context of a bilinear spontaneous RPV model.

In this paper, we study prompt multilepton and/or multijet signatures of stop/sbottom LSPs with LH or LQD RPV couplings. In addition to leptoquark searches, we apply various other RPC and RPV SUSY searches with multileptons (and possibly missing energy). Our emphasis is on the latest collider constraints coming from various search results combined (also in comparison with RPC model constraints), as well as comparisons and contrasts of

* ejchun@kias.re.kr

† nejsh21@gmail.com

‡ hmlee@cau.ac.kr

§ s.park@skku.edu

¹Note that the dimension-5 *B* and *L* violating operator $LQ_1 Q_2 Q_3$, which is R-parity even, is assumed to be highly suppressed in addition.

the sbottom LSP versus the stop LSP and LQD versus LH couplings at colliders.

Recently, the CMS has also reported excesses in the leptoquark mass range of 600–700 GeV in both $eejj$ and $e\nu jj$ channels with 2.4σ and 2.6σ , respectively [10]. These excesses are characterized by jets from non- b quarks. On the other hand, no similar excess is observed in $\mu\mu(\nu)jj$ and $\tau\tau(\nu)jj$ channels. It is tempting to see if such observed signatures are understood by any of RPV stop/sbottom LSP decay processes. Interestingly, we find that these excesses can be accommodated in the mostly left-handed sbottom LSP scenario with appropriate LQD operators. This may have some implication on the other stop/sbottom masses from the electroweak precision data (EWPD). One can find other attempts to explain the excess in Ref. [16].

This paper is organized as follows. We start by deriving the stop/sbottom RPV vertices arising from the LH and LQD couplings and reviewing their implication to the neutrino mass matrix, and then we set up benchmark models specified by various LH and LQD couplings in Sec. II. Various LHC 7 + 8 TeV results are reinterpreted to constrain these benchmark models in Sec. III. Several qualitatively different models are considered and dedicated searches are proposed. The latest constraints are presented here. Section IV addresses the issue of accommodating the recently observed mild excesses in the CMS leptoquark searches in our context, and possible implications of the successful accommodation to EWPD constraints. Finally we conclude in Sec. V.

II. MODELS WITH LH AND LQD RPV

A. General consideration

As mentioned, we consider the LH and LQD operators relevant for the stop and sbottom LSP decays:

$$W_{\text{RPV}} = \epsilon_i \mu L_i H_u + \lambda'_{ijk} L_i Q_j D_k^c. \quad (2)$$

LH: Let us first derive the stop and sbottom couplings arising from the bilinear LH RPV. For this, we need to include also soft SUSY breaking bilinear terms,

$$V_{\text{soft,LH}} = B_i \tilde{L}_i H_u + m_{L_i H_d}^2 \tilde{L}_i H_d^\dagger + \text{H.c.}, \quad (3)$$

which generate the vacuum expectation value (VEV) of a sneutrino field $\tilde{\nu}_i$ parametrized as $\langle \tilde{\nu}_i \rangle \equiv a_i \langle H_d \rangle$ with $a_i = (B_i t_\beta + m_{L_i H_d}^2) / m_{\tilde{\nu}_i}^2$. Here $t_\beta \equiv \tan \beta$ is the ratio between two Higgs VEVs: $t_\beta = \langle H_u^0 \rangle / \langle H_d^0 \rangle$. The bilinear couplings ϵ_i and a_i induce mixing masses between neutrinos (charged leptons) and neutralinos (charginos) and thereby nonvanishing neutrino masses as well as effective RPV couplings of the stop and sbottom LSP of our interest. To see this, it is convenient to diagonalize away first these mixing masses as discussed in the second paper of Ref. [6].

The relevant approximate diagonalizations valid in the limit of $\epsilon_i, a_i \ll 1$ as required by tiny neutrino masses are as follows.

- (i) Neutrino-neutralino diagonalization:

$$\begin{pmatrix} \nu_i \\ \chi_j^0 \end{pmatrix} \longrightarrow \begin{pmatrix} \nu_i - \theta_{ik}^N \chi_k^0 \\ \chi_j^0 + \theta_{lj}^N \nu_l \end{pmatrix}, \quad (4)$$

where (ν_i) and (χ_j^0) represent three neutrinos $(\nu_e, \nu_\mu, \nu_\tau)$ and four neutralinos $(\tilde{B}, \tilde{W}_3, \tilde{H}_d^0, \tilde{H}_u^0)$ in the flavor basis, respectively. The rotation elements θ_{ij}^N are given by

$$\begin{aligned} \theta_{ij}^N &= \xi_i c_j^N c_\beta - \epsilon_i \delta_{j3} \quad \text{and} \\ (c_j^N) &= \frac{M_Z}{F_N} \left(\frac{s_W M_2}{c_W^2 M_1 + s_W^2 M_2}, -\frac{c_W M_1}{c_W^2 M_1 + s_W^2 M_2}, \right. \\ &\quad \left. -s_\beta \frac{M_Z}{\mu}, c_\beta \frac{M_Z}{\mu} \right), \end{aligned} \quad (5)$$

where $\xi_i \equiv a_i - \epsilon_i$ and $F_N = M_1 M_2 / (c_W^2 M_1 + s_W^2 M_2) + M_Z^2 s_{2\beta} / \mu$. Here $s_W = \sin \theta_W$ and $c_W = \cos \theta_W$ with the weak mixing angle θ_W .

- (ii) Charged-lepton-chargino diagonalization:

$$\begin{aligned} \begin{pmatrix} e_i \\ \chi_j^- \end{pmatrix} &\rightarrow \begin{pmatrix} e_i - \theta_{ik}^L \chi_k^- \\ \chi_j^- + \theta_{lj}^L e_l \end{pmatrix}; \\ \begin{pmatrix} e_i^c \\ \chi_j^+ \end{pmatrix} &\rightarrow \begin{pmatrix} e_i^c - \theta_{ik}^R \chi_k^+ \\ \chi_j^+ + \theta_{lj}^R e_l^c \end{pmatrix}, \end{aligned} \quad (6)$$

where e_i and e_i^c denote the left-handed charged leptons and antileptons, $(\chi_j^-) = (\tilde{W}^-, \tilde{H}^-)$ and $(\chi_j^+) = (\tilde{W}^+, \tilde{H}^+)$. The rotation elements $\theta_{ij}^{L,R}$ are given by

$$\begin{aligned} \theta_{ij}^L &= \xi_i c_j^L c_\beta - \epsilon_i \delta_{j2}, \quad \theta_{ij}^R = \frac{m_i^c}{F_C} \xi_i c_j^R c_\beta \quad \text{and} \\ (c_j^L) &= -\frac{M_W}{F_C} \left(\sqrt{2}, 2s_\beta \frac{M_W}{\mu} \right), \\ (c_j^R) &= -\frac{M_W}{F_C} \left(\sqrt{2} \left(1 - \frac{M_2}{\mu} t_\beta \right), \frac{M_2^2 c_\beta^{-1}}{\mu M_W} + 2 \frac{M_W}{\mu} c_\beta \right), \end{aligned} \quad (7)$$

and $F_C = M_2 + M_W^2 s_{2\beta} / \mu$.

After these diagonalizations, we get the following RPV vertices of stops:

$$\begin{aligned}
-\mathcal{L} = & \tilde{t}_L \bar{t} (\kappa_{L\nu_i}^t P_L + \kappa_{R\nu_i}^t P_R) \nu_i \\
& + \tilde{t}_R \bar{t} (\rho_{L\nu_i}^t P_L + \rho_{R\nu_i}^t P_R) \nu_i + \text{H.c.} \\
& + \tilde{t}_L \bar{b} (\kappa_{Le_i}^t P_L + \kappa_{Re_i}^t P_R) e_i \\
& + \tilde{t}_R \bar{b} (\rho_{Le_i}^t P_L + \rho_{Re_i}^t P_R) e_i + \text{H.c.},
\end{aligned}$$

where $\kappa_{L\nu_i}^t = y_t c_4^N \xi_i c_\beta$,

$$\begin{aligned}
\kappa_{R\nu_i}^t &= \left(\frac{\sqrt{2}}{6} g' c_1^N + \frac{1}{\sqrt{2}} g c_2^N \right) \xi_i c_\beta, \\
\rho_{L\nu_i}^t &= \frac{2\sqrt{2}}{3} g' c_1^N \xi_i c_\beta, \quad \rho_{R\nu_i}^t = y_t c_4^N \xi_i c_\beta, \\
\kappa_{Le_i}^t &= -y_b c_2^L \xi_i c_\beta + y_b \epsilon_i, \quad \kappa_{Re_i}^t = g \frac{m_i^e}{F_C} c_1^R \xi_i c_\beta, \\
\rho_{Le_i}^t &= 0, \quad \rho_{Re_i}^t = -y_t \frac{m_i^e}{F_C} c_2^R \xi_i c_\beta.
\end{aligned} \quad (8)$$

Similarly, the sbottom RPV vertices are given by

$$\begin{aligned}
-\mathcal{L} = & \tilde{b}_L \bar{b} (\kappa_{L\nu_i}^b P_L + \kappa_{R\nu_i}^b P_R) \nu_i \\
& + \tilde{b}_R \bar{b} (\rho_{L\nu_i}^b P_L + \rho_{R\nu_i}^b P_R) \nu_i + \text{H.c.} \\
& + \tilde{b}_L \bar{t} (\kappa_{Le_i}^b P_L + \kappa_{Re_i}^b P_R) e_i \\
& + \tilde{b}_R \bar{t} (\rho_{Le_i}^b P_L + \rho_{Re_i}^b P_R) e_i + \text{H.c.},
\end{aligned}$$

where $\kappa_{L\nu_i}^b = y_b c_3^N \xi_i c_\beta - y_b \epsilon_i$,

$$\begin{aligned}
\kappa_{R\nu_i}^b &= \left(\frac{\sqrt{2}}{6} g' c_1^N - \frac{1}{\sqrt{2}} g c_2^N \right) \xi_i c_\beta, \\
\rho_{L\nu_i}^b &= -\frac{\sqrt{2}}{3} g' c_1^N \xi_i c_\beta, \quad \rho_{R\nu_i}^b = y_b c_3^N \xi_i c_\beta - y_b \epsilon_i, \\
\kappa_{Le_i}^b &= -y_t \frac{m_i^e}{F_C} c_2^R \xi_i c_\beta, \quad \kappa_{Re_i}^b = g \frac{m_i^e}{F_C} c_1^R \xi_i c_\beta, \\
\rho_{Le_i}^b &= 0, \quad \rho_{Re_i}^b = -y_b c_2^L \xi_i c_\beta + y_b \epsilon_i.
\end{aligned} \quad (9)$$

LQD: It is straightforward to get the stop and sbottom RPV vertices coming from the trilinear RPV couplings, λ'_{ijk} with j or $k = 3$:

$$\begin{aligned}
-\mathcal{L} = & \lambda'_{i33} (\tilde{b}_L \bar{b} P_L \nu_i + \tilde{b}_R \bar{b} P_R \nu_i - \tilde{t}_L \bar{b} P_L e_i - \tilde{b}_R \bar{t} P_R e_i) + \text{H.c.} \\
& + \lambda'_{ij3} (\tilde{b}_R \bar{d}_j P_R \nu_i - \tilde{b}_R \bar{u}_j P_R e_i) + \text{H.c.} \\
& + \lambda'_{i3k} (\tilde{b}_L \bar{d}_k P_L \nu_i - \tilde{t}_L \bar{d}_k P_L e_i) + \text{H.c.}
\end{aligned} \quad (10)$$

When the LH and LQD RPV are allowed, their couplings can contribute to generate neutrino mass matrix components, respectively, at tree and one-loop (see Fig. 1) as follows [4–6]:

$$m_{\nu,ij}^{\text{tree}} = \frac{M_Z^2}{F_N} \xi_i \xi_j c_\beta^2, \quad (11)$$

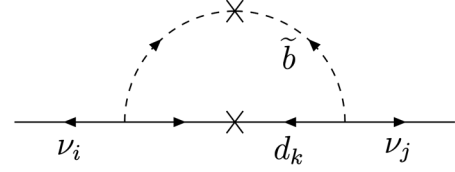


FIG. 1. Feynman diagrams responsible for neutrino mass generation, $m_{\nu,ij}$, through light sbottoms and LQD couplings $\lambda'_{ik3}\lambda'_{j3k}$.

$$m_{\nu,ij}^{\text{loop}} = \sum_{k=1}^3 \frac{3}{16\pi^2} (\lambda'_{ik3}\lambda'_{j3k} + \lambda'_{i3k}\lambda'_{jk3}) \frac{m_{d_k} m_b X_b}{m_{b_2}^2 - m_{b_1}^2} \ln \frac{m_{b_2}^2}{m_{b_1}^2}, \quad (12)$$

where $m_b X_b$ is the sbottom mixing mass-squared and only sbottom contributions are included assuming $m_{\tilde{b}} \ll m_{\tilde{d}_k}$ for $k = 1, 2$. A complete one-loop calculation can be found in Refs. [5,6]. In the case of the neutralino LSP, the RPV signatures correlated with the neutrino mixing angles have been extensively studied [17–19], as well as in the split SUSY [20]. Similar studies are worthwhile in the case of the stop/sbotttom LSP as well. We leave this issue to a future work.

From the expressions in Eqs. (11), (12), the LH and LQD couplings are constrained by the measured values of tiny neutrino masses. As a rough estimate, the following bilinear and trilinear couplings are required to generate the neutrino mass components of $m_{\nu,ii} = 0.01$ eV:

$$|\xi_i c_\beta| \approx 10^{-6}, \quad (13)$$

$$|\lambda'_{ik3}\lambda'_{i3k}|^{1/2} \approx 3.4 \times 10^{-3} \sqrt{\frac{m_d}{m_{d_k}}}, \quad (14)$$

taking $F_N = X_b = \sqrt{(m_{b_2}^2 - m_{b_1}^2) / \ln(m_{b_2}^2 / m_{b_1}^2)} = 1$ TeV. These coupling sizes are small enough that they do not affect production rates and do not make resonances broader than experimental resolutions so that collider physics is mostly independent on them. Nevertheless, they are large enough to allow prompt decays of squark LSPs.

B. Benchmark models

We now introduce three benchmark models. Sbottom and stop LSPs decay to either first- or second-generation leptons. Model names imply the involved RPV interactions and subscripts imply lepton and/or quark generations.

In the presence of the mixing between left-handed and right-handed stops/sbottoms, we can write the stop/sbotttom mass eigenstates, \tilde{q}_1 and \tilde{q}_2 , with $q = t, b$:

$$\begin{aligned}
\tilde{q}_L &= \cos \theta_{\tilde{q}} \tilde{q}_1 - \sin \theta_{\tilde{q}} \tilde{q}_2, \\
\tilde{q}_R &= \sin \theta_{\tilde{q}} \tilde{q}_1 + \cos \theta_{\tilde{q}} \tilde{q}_2,
\end{aligned} \quad (15)$$

where $\theta_{\tilde{q}}$ is the squark mixing angle. We are interested in the RPV vertices of the lightest stop (\tilde{t}_1) or sbottom (\tilde{b}_1).

LH_i: Stop and sbottom decay modes are $\tilde{b}_1 \rightarrow e_i t, \nu_i b$ and $\tilde{t}_1 \rightarrow e_i b, \nu_i t$, and the branching fractions for the charged lepton modes are given by (ignoring top and bottom masses)

$$\beta_{\tilde{b}} \equiv \text{BR}(\tilde{b}_1 \rightarrow e_i t) \approx \frac{\sin^2 \theta_{\tilde{b}} |\rho_{Re_i}^b|^2}{|\kappa_{L\nu_i}^b|^2 + \cos^2 \theta_{\tilde{b}} |\kappa_{R\nu_i}^b|^2 + \sin^2 \theta_{\tilde{b}} |\rho_{L\nu_i}^b|^2 + \sin^2 \theta_{\tilde{b}} |\rho_{Re_i}^b|^2}, \quad (16)$$

$$\beta_{\tilde{t}} \equiv \text{BR}(\tilde{t}_1 \rightarrow e_i b) \approx \frac{\cos^2 \theta_{\tilde{t}} |\kappa_{Le_i}^t|^2}{|\kappa_{L\nu_i}^t|^2 + \cos^2 \theta_{\tilde{t}} |\kappa_{R\nu_i}^t|^2 + \sin^2 \theta_{\tilde{t}} |\rho_{L\nu_i}^t|^2 + \cos^2 \theta_{\tilde{t}} |\kappa_{Le_i}^t|^2}, \quad (17)$$

where we neglect the terms suppressed by m_i^e/F_C . As the stop or the sbottom is the LSP, it is expected to have $M_Z \ll \mu$ and thus $|c_{3,4}^N, c_2^{L,R}| \ll |c_{1,2}^N, c_1^{L,R}|$, which leads to

$$\beta_{\tilde{b}} \approx \frac{\sin^2 \theta_{\tilde{b}} |y_b \epsilon_i|^2}{[\cos^2 \theta_{\tilde{b}} |\frac{\sqrt{2}}{6} g' c_1^N - \frac{1}{\sqrt{2}} g c_2^N|^2 + \sin^2 \theta_{\tilde{b}} |\frac{\sqrt{2}}{3} g' c_1^N|^2] |\xi_i c_\beta|^2 + (1 + \sin^2 \theta_{\tilde{b}}) |y_b \epsilon_i|^2}, \quad (18)$$

$$\beta_{\tilde{t}} \approx \frac{\cos^2 \theta_{\tilde{t}} |y_b \epsilon_i|^2}{[\cos^2 \theta_{\tilde{t}} |\frac{\sqrt{2}}{6} g' c_1^N + \frac{1}{\sqrt{2}} g c_2^N|^2 + \sin^2 \theta_{\tilde{t}} |\frac{2\sqrt{2}}{3} g' c_1^N|^2] |\xi_i c_\beta|^2 + \cos^2 \theta_{\tilde{t}} |y_b \epsilon_i|^2}. \quad (19)$$

Note that the LH model becomes effectively equivalent to the LQD_{i33} model with $\lambda'_{i33} \equiv \epsilon_i y_b$ (see below) in the limit of vanishing ξ_i .

LQD_{i33}: Only $\lambda'_{i33} \neq 0$ is assumed to allow the decay modes $\tilde{b}_1 \rightarrow e_i t, \nu_i b$ or $\tilde{t}_1 \rightarrow e_i b$. Thus, the sbottom and stop decay branching ratios for the charged lepton modes are

$$\beta_{\tilde{b}} \equiv \text{BR}(\tilde{b}_1 \rightarrow e_i t) = \frac{\sin^2 \theta_{\tilde{b}}}{1 + \sin^2 \theta_{\tilde{b}}}, \quad (20)$$

$$\beta_{\tilde{t}} \equiv \text{BR}(\tilde{t}_1 \rightarrow e_i b) = 1. \quad (21)$$

LQD_{ij3+i3j}: Only $\lambda'_{ij3+i3j} \neq 0$ is assumed to allow $\tilde{b}_1 \rightarrow e_i u_j, \nu_i d_j$ or $\tilde{t}_1 \rightarrow e_i d_j$. The sbottom and stop branching ratios for the charged lepton modes are

$$\beta_{\tilde{b}} \equiv \text{BR}(\tilde{b}_1 \rightarrow e_i u_j) = \frac{\sin^2 \theta_{\tilde{b}} |\lambda'_{ij3}|^2}{\cos^2 \theta_{\tilde{b}} |\lambda'_{i3j}|^2 + 2 \sin^2 \theta_{\tilde{b}} |\lambda'_{ij3}|^2}, \quad (22)$$

$$\beta_{\tilde{t}} \equiv \text{BR}(\tilde{t}_1 \rightarrow e_i d_j) = 1. \quad (23)$$

The first two models, LH_i and LQD_{i33}, involve heavy quarks (tops and bottoms) in the final states while only light quarks are produced in the LQD_{ij3+i3j} model. In the following section we will investigate the LHC searches and bounds on the stop/sbotttom LSP, concentrating on the first two generations of leptoquark features involving e and μ in the final state. Considering the third-generation

leptoquark searches involving τ in the final state [9,12], one expects to get less stringent limits.

III. LHC SEARCHES AND BOUNDS

Let us first consider how the sbottom LSP can be constrained at the LHC. Sbottom pair productions in the LH₁ and LQD₁₃₃ models leave the final states:

$$\tilde{b}_1 \tilde{b}_1^* \rightarrow bb\nu\nu, tbe\nu, ttee. \quad (24)$$

The $bb\nu\nu$ is constrained by RPC sbottom searches through $\tilde{b}_1 \rightarrow b\chi_1^0$ with the massless LSP, hence $b\bar{b}$ + missing transverse energy (MET). The existing strongest bound on the sbottom mass is 725 GeV from CMS 19.4/fb [21]. The $tbe\nu$ can be constrained from the $e\nu jj$ searches of first-generation leptoquarks [10]—the CMS analysis uses the two hardest jets of any flavor. Note that the sbottom and the leptoquark have the same quantum numbers as the color triplet, and their production rates are almost identical, as dictated by QCD interactions. So it is appropriate to use this result to extract bounds on sbottoms. The $ttee$ can be constrained from the $eejj$ searches of leptoquarks and additionally from multilepton ($\geq 3\ell$) RPV LLE searches [22]. We comment on other searches in the Appendix.

We recast these search results to exclusion bounds on the sbottom in the left panel of Fig. 2; we refer to the Appendix for how we obtain these bounds. The same bounds apply to both LQD₁₃₃ and LH₁ as they predict the same final states. Large $\beta_{\tilde{b}}$ is constrained from the $eejj$ and the multilepton RPV searches, whereas small $\beta_{\tilde{b}}$ is constrained from the RPC sbottom search. In general, sbottoms lighter than

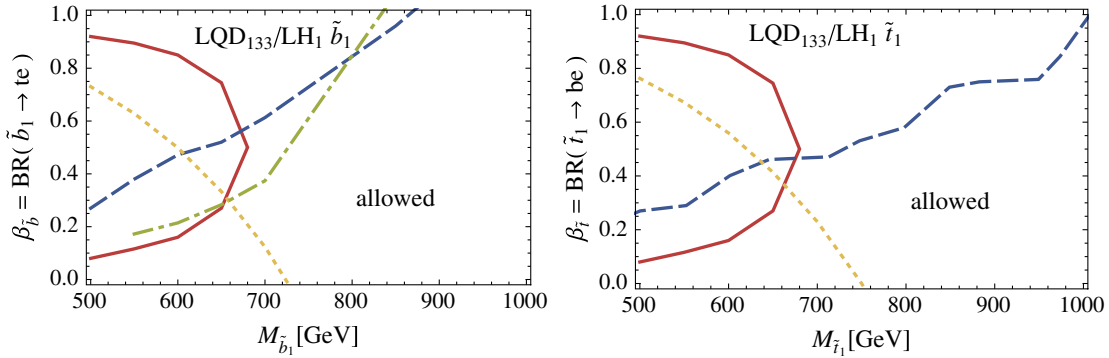


FIG. 2 (color online). 95% C.L. exclusion plots for the sbottom LSP (left) and the stop LSP (right) from CMS leptoquark searches in $eejj$ (blue dashed) and $evjj$ (red solid) channels. Also shown are CMS RPC sbottom and stop searches (yellow dotted) in $b\bar{b} + \text{MET}$ and $t\bar{t} + \text{MET}$ channels. For sbottoms, CMS multilepton ($\geq 3\ell$) RPV search constraints are shown additionally (green dot-dashed). The region to the left of each line is excluded. The bounds are equally applicable to LH_1 and LQD_{133} models (except that $\beta_{\tilde{t}} = 1$ for the stop LSP with LQD_{133}).

about 660 GeV are excluded by at least one of those searches.

We now turn to the stop LSP. Stop pairs in the LH_1 and LQD_{133} models decay as

$$\tilde{t}_1 \tilde{t}_1^* \rightarrow tt\nu, tbe\nu, bbee, \quad (25)$$

where the first two modes are not allowed in the LQD_{133} model; see Eqs. (20) and (21). The $tt\nu$ channel is constrained by RPC stop searches through $\tilde{t}_1 \rightarrow t\chi_1^0$ with the massless LSP. The existing strongest bound is 750 GeV from CMS 19.5/fb [23]. The remaining decay modes, $tbe\nu$ and $bbee$, can be constrained from the $evjj$ and $eejj$ searches of first-generation leptoquarks [10]. Note that the stop also has the same quantum numbers as leptoquarks. Unlike sbottoms, stop pairs do not lead to final states with more than two leptons. Recasting these search results to exclusion bounds on the stop, we obtain the right panel of Fig. 2. Similarly to the sbottom case, stops lighter than about 660 GeV are excluded.

There is one notable difference between the sbottom LSP and the stop LSP. Sbottom pairs decay to $ttee$, while stop pairs decay to $bbee$. Tops produce more jets, and each jet becomes softer as decay products share the energy-momentum of sbottoms. Thus the acceptance under leptoquark search cuts gets lower. The $eejj$ exclusion bound (blue dashed) on sbottoms (the left panel of Fig. 2) is indeed weaker than that on stops (the right panel of Fig. 2). Likewise, the $evjj$ bound (red solid) in Fig. 2 is also weaker than the official $evjj$ bound on the leptoquark model in Ref. [10]; the reported bound reaches up to 850 GeV higher than 680 GeV here.

Most notably, the invariant mass of the ej pair, $m_{ej,\text{min}}$, does not reconstruct the sbottom mass. In Fig. 3, we contrast the invariant mass spectrum for the sbottom LSP and the stop LSP. We choose the presumably correct ej pair according to the CMS leptoquark analysis; the pair giving smaller invariant mass difference is selected. The m_{ej} from sbottoms have a broader spectrum and the peak formed at a lower mass because not all top decay products

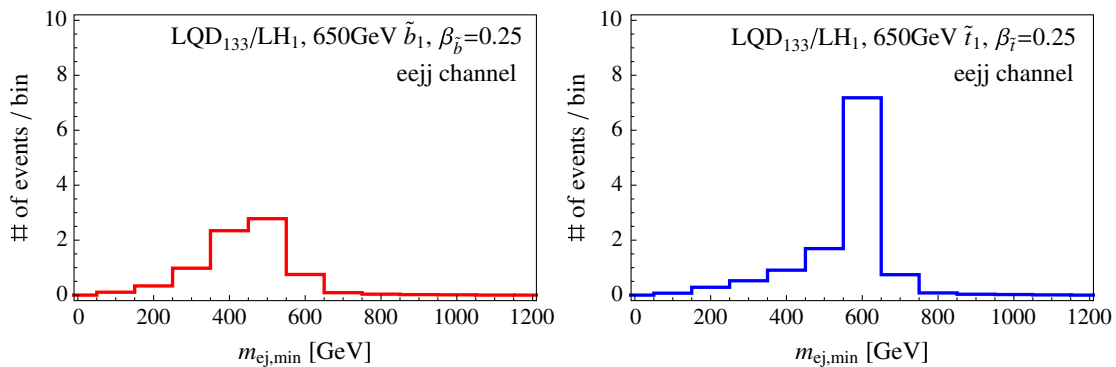


FIG. 3 (color online). Invariant mass, $m_{ej,\text{min}}$, from 650 GeV sbottom (left) or stop (right) pairs decaying to $eejj$ channel via LH_1 or LQD_{133} RPV couplings. CMS leptoquark search cuts are applied except for the cut on the invariant mass. 19.6/fb is assumed. $\beta_{\tilde{b},\tilde{t}} = 0.25$ is chosen for illustration.

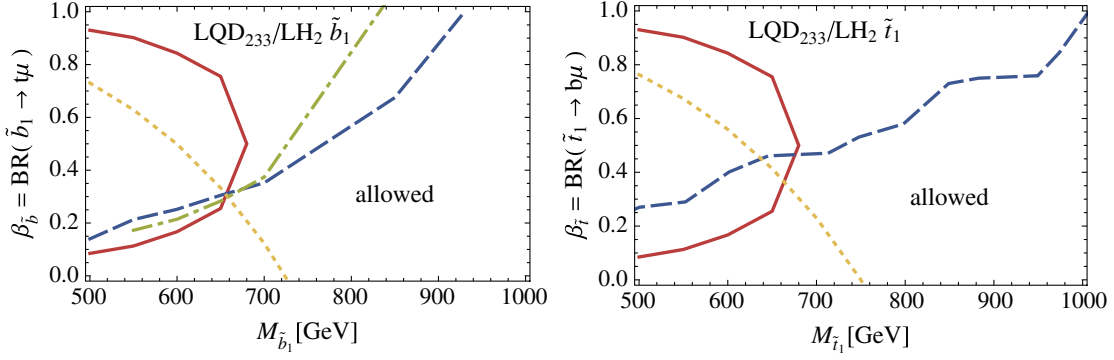


FIG. 4 (color online). Same as in Fig. 2 but the μ channel results of CMS leptoquark searches [11] are used for the red solid and blue dashed lines, which constrain the LH_2 and LQD_{233} models.

are included. It will be useful to measure this characteristic difference in the future searches.

Therefore, potentially significant improvements in the third-generation squark LSP searches can be achieved with b -taggings and/or top reconstructions. With 20/fb of data, $8.1 \text{ fb} \times 20/\text{fb} \approx 160$ pairs of 700 GeV sbottoms are produced, and much better bounds are beginning to be statistically limited. In any case, 160 is still a reasonably large number, and more dedicated searches implementing b -tagging and/or top reconstruction are certainly worthwhile.

We can repeat the same analysis in the LH_2 and LQD_{233} models allowing sbottom and stop LSP decays to μ , and apply the CMS second-generation leptoquark searches [11]. The resulting bounds are shown in Fig. 4. Compared to the $eejj$ search, the $\mu\mu jj$ search is somewhat more stringent partly because μ is more accurately measured and cleaner—compare blue dashed lines in the left panels of Fig. 2 and Fig. 4. On the other hand, $\mu\nu jj$ results are similar to $e\nu jj$ results (red solid lines). To summarize, again, third-generation squark LSPs lighter than about 660 GeV are generally excluded.

Finally, the $LQD_{ij3+i3j}$ models with $i, j = 1, 2$ are equivalent to the leptoquark models and the current search results can be directly applied to constrain the sbottom/stop LSP mass. For the case with large BR into neutrinos, searches of light squarks in multijet plus MET will apply similarly to small β regions discussed above. Overall, third-generation squark LSPs in this case are also similarly or only slightly more strongly constrained than the cases discussed above. We comment that our recast bounds in Figs. 2 and 4 are applicable to more general models if production cross sections and decay modes are close to the ones in the models considered here.

IV. THE OBSERVED LEPTOQUARK EXCESS FROM SBOTTOM DECAYS

The CMS leptoquark analysis has recently reported excesses in 650 GeV leptoquark searches in both $eejj$ and $e\nu jj$ channels [10]. The excesses are claimed to be 2.4

and 2.6 σ significant, respectively. The excesses disappear when a b -jet is required, and no similar excess is observed in searches with μ [11] and τ [12]. In this section, we discuss how our third model, $LQD_{113+131}$, can fit the excesses.

A. Sbottoms as leptoquarks

Sbottom pairs in the $LQD_{113+131}$ model decay as

$$\tilde{b}_1 \tilde{b}_1^* \rightarrow d d \nu \nu, d u e \nu, u u e e, \quad (26)$$

with $\text{BR} = (1 - \beta)^2, 2\beta(1 - \beta)$ and β^2 , respectively. This model is identical to the first-generation leptoquark model considered in the CMS analysis except that β is given differently by Eq. (22) in our model. The best fit is allegedly reported to be with 650 GeV and $\beta = 0.075$. Our model can accommodate this by the decay of sbottom LSPs. By simply assuming $\lambda'_{113} = \lambda'_{131}$ as an example, we can extract more specific information on the underlying parameters. Then, $\beta = \sin^2 \theta_{\tilde{b}} / (1 + \sin^2 \theta_{\tilde{b}}) \leq 0.5$ is now bounded from above. The best-fit value, $\beta = 0.075$, requires $\sin^2 \theta_{\tilde{b}} = 0.081$, meaning that the sbottom LSP is mostly left-handed. The constraint from the electroweak precision test is briefly discussed in the next subsection.

The $m_{ej,\min}$ invariant mass spectrum is also scrutinized in the CMS analysis. So far, no sharp peak is observed unlike the expectation from leptoquark decays. As compared to our previous two models, the $LQD_{113+131}$ does not involve top quarks and would also predict the same sharp peak in the invariant mass as the leptoquark model does. See Fig. 5 for the comparison of the model prediction and data—no clear resonancelike structure is seen in the data, but the model prediction is not significantly different from data yet.

Our interpretation of the sbottom LSP in the $LQD_{113+131}$ model as a leptoquark of 650 GeV responsible for the mild CMS excesses requires the corresponding couplings, λ'_{113} and λ'_{131} , to dominate over other sbottom LSP RPV couplings if any. These couplings may be relevant to the generation of the observed neutrino masses and mixing as discussed in Eqs. (13)–(14). In this case, one could have

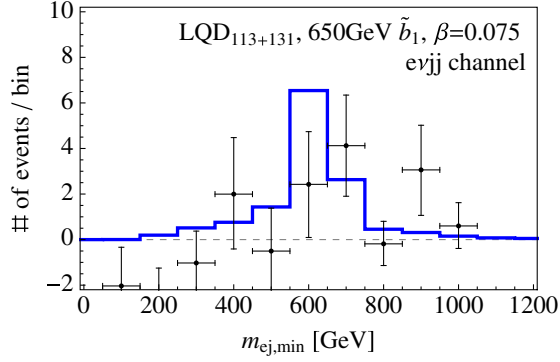


FIG. 5 (color online). The invariant mass, $m_{ej,\min}$, from 650 GeV sbottom pairs decaying to the $evjj$ channel via $LQD_{113+131}$ RPV couplings. CMS leptquark search cuts are applied except for the cut on the invariant mass. 19.6/fb is assumed. A small $\beta = 0.075$, giving a good fit to data, is chosen. The data with SM predictions subtracted are taken from CMS results in Ref. [10].

$\lambda'_{113} \sim \lambda'_{131} \sim 10^{-3}$ to produce (mainly) the (11) component of the observed neutrino mass matrix. Then, the other components can come from smaller bilinear RPV couplings $\xi_i c_\beta \sim 10^{-6}$ and/or trilinear couplings, e.g., $\lambda'_{i33} \sim 10^{-4}$ to produce $m_{\nu,ij}^{\text{tree}} \propto \xi_i \xi_j c_\beta^2$ and/or $m_{\nu,ij}^{\text{loop}} \propto \lambda'_{i33} \lambda'_{j33}$. In this

scenario, the sbottom LSP can have additional but suppressed decay modes in the μ and τ channels through $\xi_i \ll \lambda'_{j33} \ll \lambda'_{113,131}$ ($i, j = 2, 3$) which may provide a test of the model. Of course, the neutrino mass components can come mainly from the LLE couplings, e.g., $m_{\nu,ij}^{\text{loop}} \propto \lambda_{i33} \lambda_{j33}$, which has no impact on the sbottom LSP phenomenology.

B. Electroweak precision data and stop masses

The mostly left-handed sbottom solution obtained in the previous subsection may imply that other stops (and/or sbottoms) are also light; otherwise, the model is inconsistent with the electroweak precision data (EWPD). The possible other light particles can provide additional collider constraints on the model. Indeed, it has been shown that the EWPD can give important constraints on the stop masses and mixing angles in combination with the RPC searches of sbottoms [24].

The deviation from the custodial symmetry in the SM is bounded to [25]

$$(\Delta\rho)^\pm = (\rho_0)_{m_t=125 \text{ GeV}} - 1 = (4.2 \pm 2.7) \times 10^{-4}. \quad (27)$$

The sbottom and stop contribution to the ρ parameter [26] is

$$\begin{aligned} \Delta\rho_0^{\text{SUSY}} = & \frac{3G_\mu}{8\sqrt{2}\pi^2} [-\sin^2\theta_t \cos^2\theta_b F_0(m_{t_1}^2, m_{t_2}^2) - \sin^2\theta_b \cos^2\theta_t F_0(m_{b_1}^2, m_{b_2}^2) + \cos^2\theta_t \cos^2\theta_b F_0(m_{t_1}^2, m_{b_1}^2) \\ & + \cos^2\theta_t \sin^2\theta_b F_0(m_{t_1}^2, m_{b_2}^2) + \sin^2\theta_t \cos^2\theta_b F_0(m_{t_2}^2, m_{b_1}^2) + \sin^2\theta_t \sin^2\theta_b F_0(m_{t_2}^2, m_{b_2}^2)], \end{aligned} \quad (28)$$

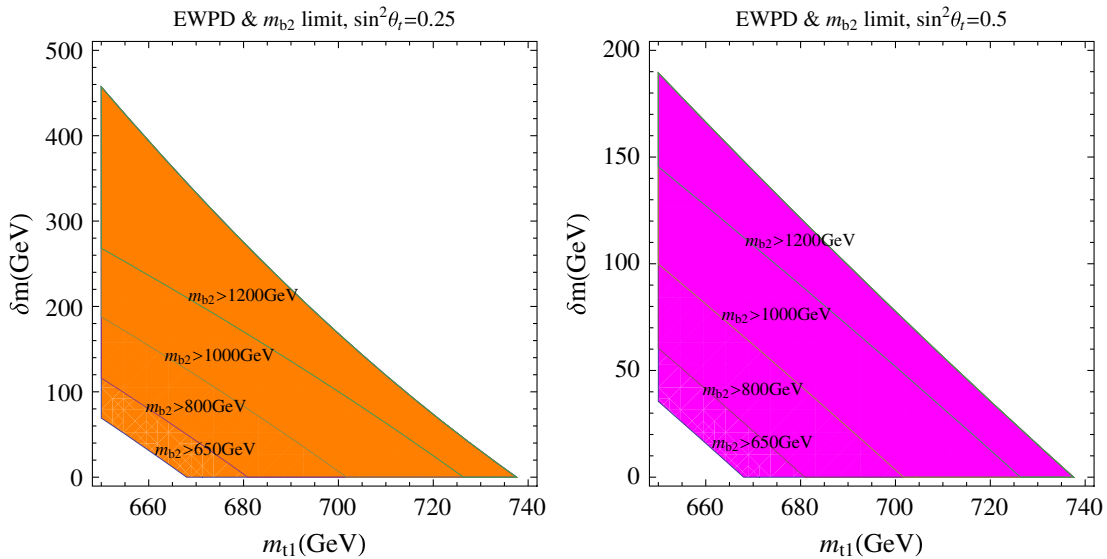


FIG. 6 (color online). The EWPD constraints on stop and heavy sbottom masses for the best-fit parameters, with 650 GeV sbottom LSP and $\sin^2\theta_b = 0.081$. Here, $\delta m \equiv m_{t_2} - m_{t_1}$ is the stop mass splitting. Lighter stop mass is bounded by EWPD and the stop mass splitting scales up as the bound on the heavier sbottom mass increases. In both figures, $\tan\beta = 10$ is chosen.

where F_0 is defined by

$$F_0[x, y] = x + y - \frac{2xy}{x-y} \log \frac{x}{y}. \quad (29)$$

From the mass terms for stops and sbottoms, we can infer the following relation between physical squark masses and mixing angles:

$$\begin{aligned} & \sin^2 \theta_{\tilde{b}} m_{\tilde{b}_2}^2 + \cos^2 \theta_{\tilde{b}} m_{\tilde{b}_1}^2 \\ &= \cos^2 \theta_{\tilde{t}} m_{\tilde{t}_1}^2 + \sin^2 \theta_{\tilde{t}} m_{\tilde{t}_2}^2 - m_{\tilde{t}}^2 - m_{\tilde{W}}^2 \cos(2\beta) + m_{\tilde{b}}^2. \end{aligned} \quad (30)$$

In Fig. 6, we show bounds on the masses of other sbottoms and stops by assuming the best-fit parameters, $m_{\tilde{b}_1} = 650$ GeV and $\sin^2 \theta_{\tilde{b}} = 0.081$, chosen in the previous subsection. Although the EWPD bound depends on various other parameters including the stop mixing angle, the lighter stop mass is bounded up to about 740 GeV and the stop mass splitting is bounded up to about 190 GeV for a maximal stop mixing. In particular, when the collider limit on the heavier sbottom mass increases, the lighter stop mass and the stop mass splitting tend to get larger so the allowed parameter space in the stop sector is reduced.

The 125 GeV Higgs mass would require stop masses of 500–800 GeV for a maximal stop mixing or stop masses above 3 TeV for a zero stop mixing [27]. Thus, in the case of a small stop mixing, the Higgs mass condition would be incompatible with EWPD. On the other hand, for a maximal stop mixing, the stop masses required for the Higgs mass can constrain the parameter space further. When there is a new dynamics for enhancing the Higgs mass such as a singlet chiral superfield, we may take the EWPD in combination with a sbottom mass limit to be a robust bound on stop masses.

V. SUMMARY AND CONCLUSION

Through LH and LQD RPV couplings, the third-generation squark LSP can decay to leptons and jets. Jet + MET final states are constrained by conventional RPC SUSY searches, and multilepton(+jets) + MET final states are constrained from leptoquark searches as well as multilepton RPV searches. We found that the sbottom and the stop LSP decaying to e or μ are similarly well constrained up to about 0.66–1 TeV depending on leptonic branching fractions. When the sbottom decays to a top quark and an electron as in the LH_i and LQD_{i33} models, the bounds are slightly weaker as each top decay product is softer and not all is used in the analyses. The resulting characteristically different m_{e_j} invariant mass spectra can distinguish the models. A more dedicated search for this case can be pursued by implementing b -taggings and/or top reconstructions. The bounds on μ final states are somewhat stronger than those on e final states so that a wider region of

parameter space above 660 GeV is excluded for the LH_2 and LQD_{233} models. Lastly, we proposed the $LQD_{113+131}$ model with mostly left-handed sbottom LSPs as a good fit to the recently observed mild leptoquark excesses, and we discussed its possible implications on the masses of other stops and sbottoms in view of the EWPD and the 125 GeV Higgs mass.

ACKNOWLEDGMENTS

We thank Suyong Choi for helpful comments and Adam Martin for comments on Fig. 5. E. J. C. is supported by the NRF grant funded by the Korea government (MSIP) (Grant No. 2009-0083526) through KNRC at Seoul National University. S. J. is supported in part by the NRF Grant No. 2013R1A1A2058449. H. M. L. is supported in part by the Basic Science Research Program through the NRF Grant No. 2013R1A1A2007919 and by the Chung-Ang University Research Grants in 2014. S. C. P. is supported by the Basic Science Research Program through the NRF Grant No. NRF-2013R1A1A2064120.

APPENDIX: BOUND ESTIMATION

Here we summarize how we reinterpret LHC results to obtain exclusion bounds on our models. We use the next-to-leading order sbottom production cross sections in Refs. [28,29].

The $bb\nu\nu$ final states are constrained from RPC sbottom pair searches. Sbottoms decaying to $b\chi_1^0$ 100% are currently limited to be above 720 GeV [21]. For our given sbottom mass, by assuming the same kinematics and applying the same cut efficiencies as in RPC sbottom searches, we find the branching ratio suppression needed to make the production rate of the given $\tilde{b}_1\tilde{b}_1^* \rightarrow bb\nu\nu$ equal to that of 720 GeV sbottom pairs. We reinterpret the stop RPC searches in the $t\bar{t} + \text{MET}$ channel [23] in the same way that we constrain $t\nu\nu$ final states. For the $LQD_{113+131}$, the RPC searches of squark pairs can be similarly relevant. Interestingly, a *single* squark pair is weakly constrained from the $q\bar{q} + \text{MET}$ search [30] to be above only 570 GeV—but they can still exclude a small part of the surviving parameter space.

Various $\ell\nu jj$ final states are constrained from leptoquark searches. Leptoquark searches [10,11] display several sets of cuts (signal regions) optimized for different leptoquark masses. For the $LQD_{113+131}$ which have exactly the same kind of decay modes as leptoquarks, the official CMS exclusion bounds on leptoquarks apply equally well. For the LQD_{i33} and LH_i models which involve heavy quarks in the final states, we carry out Monte Carlo simulations (based on MADGRAPH [31], PYTHIA [32], and FASTJET [33]), estimate efficiencies under all displayed cuts and use the most constraining result. To quantify the deviation, we add statistical error, $\sqrt{S+B}$, and the reported systematic

errors in quadrature—our own 95% C.L. $\approx 1.96\sigma$ exclusion bounds on leptoquarks based on this method agree well with the official results. As different signal regions are not mutually exclusive, we do not χ^2 them.

The $t\bar{t}e$ final states can involve more than two leptons or same-sign dileptons and b -jets which are often clean. We find that the multilepton ($N_\ell \geq 3$) RPV LLE search [22] with various binned discovery cuts is most relevant to us.

We simulate all the discovery cuts with $300 < S_T < 1500$ GeV and use the most stringent result to obtain bounds. The strongest bound is usually from discovery cuts with $\geq 1b$ and $S_T \gtrsim 1000$ GeV requirements. Similar searches of same-sign dileptons plus b -jets plus multijets [34], four-lepton [35] and other $\geq 3\ell + b$ -jet searches in, e.g., Refs. [36] are less optimized for our benchmark models of about 700 GeV squarks.

-
- [1] <https://twiki.cern.ch/twiki/bin/view/AtlasPublic/SupersymmetryPublicResults>; <https://twiki.cern.ch/twiki/bin/view/CMSPublic/PhysicsResultsSUS>.
- [2] L. E. Ibanez and G. G. Ross, *Nucl. Phys.* **B368**, 3 (1992); A. H. Chamseddine and H. K. Dreiner, *Nucl. Phys.* **B458**, 65 (1996).
- [3] G. R. Farrar and P. Fayet, *Phys. Lett.* **76B**, 575 (1978).
- [4] L. J. Hall and M. Suzuki, *Nucl. Phys.* **B231**, 419 (1984); S. Dimopoulos and L. J. Hall, *Phys. Lett. B* **207**, 210 (1988); R. M. Godbole, P. Roy, and X. Tata, *Nucl. Phys.* **B401**, 67 (1993); A. S. Joshipura and M. Nowakowski, *Phys. Rev. D* **51**, 2421 (1995); M. Nowakowski and A. Pilaftsis, *Nucl. Phys.* **B461**, 19 (1996); F. M. Borzumati, Y. Grossman, E. Nardi, and Y. Nir, *Phys. Lett. B* **384**, 123 (1996); B. de Carlos and P. L. White, *Phys. Rev. D* **54**, 3427 (1996); A. Yu. Smirnov and F. Vissani, *Nucl. Phys.* **B460**, 37 (1996); R. Hempfling, *Nucl. Phys.* **B478**, 3 (1996); H. P. Nilles and N. Polonsky, *Nucl. Phys.* **B484**, 33 (1997); E. Nardi, *Phys. Rev. D* **55**, 5772 (1997); M. Drees, S. Pakvasa, X. Tata, and T. ter Veldhuis, *Phys. Rev. D* **57**, R5335 (1998); E. J. Chun, S. K. Kang, C. W. Kim, and U. W. Lee, *Nucl. Phys.* **B544**, 89 (1999); A. S. Joshipura and S. K. Vempati, *Phys. Rev. D* **60**, 09509 (1999); **60**, 111303 (1999); K. Choi, K. Hwang, and E. Chun, *Phys. Rev. D* **60**, 031301 (1999); O. Kong, *Mod. Phys. Lett. A* **14**, 903 (1999); S. Rakshit, G. Bhattacharyya, and A. Raychaudhuri, *Phys. Rev. D* **59**, 091701 (1999); R. Adhikari and G. Omanovic, *Phys. Rev. D* **59**, 073003 (1999); Y. Grossman and H. E. Haber, *Phys. Rev. D* **59**, 093008 (1999).
- [5] E. J. Chun and S. K. Kang, *Phys. Rev. D* **61**, 075012 (2000).
- [6] E. J. Chun, D. W. Jung, S. K. Kang, and J. D. Park, *Phys. Rev. D* **66**, 073003 (2002); D. W. Jung, S. K. Kang, J. D. Park, and E. J. Chun, *J. High Energy Phys.* **08** (2004) 017.
- [7] W. Buchmuller, R. Ruckl, and D. Wyler, *Phys. Lett. B* **191**, 442 (1987); **448**, 320(E) (1999).
- [8] M. Kuze and Y. Sirois, *Prog. Part. Nucl. Phys.* **50**, 1 (2003); **53**, 679 (2004).
- [9] G. Aad *et al.* (ATLAS Collaboration), *Phys. Lett. B* **709**, 158 (2012); **711**, 442(E) (2012); *Eur. Phys. J. C* **72**, 2151 (2012); G. Aad *et al.* (ATLAS Collaboration), *J. High Energy Phys.* **06** (2013) 033.
- [10] CMS Collaboration, Report No. CMS-PAS-EXO-12-041.
- [11] CMS Collaboration, Report No. CMS-PAS-EXO-12-042.
- [12] V. Khachatryan *et al.* (CMS Collaboration), *Phys. Lett. B* **739**, 229 (2014).
- [13] A. Bartl, W. Porod, M. A. Garcia-Jareno, M. B. Magro, J. W. F. Valle, and W. Majerotto, *Phys. Lett. B* **384**, 151 (1996); M. A. Diaz, D. A. Restrepo, and J. W. F. Valle, *Nucl. Phys.* **B583**, 182 (2000); H. K. Dreiner and S. Grab, *Phys. Lett. B* **679**, 45 (2009).
- [14] J. A. Evans and Y. Kats, *J. High Energy Phys.* **04** (2013) 028; S. Biswas, D. Ghosh, and S. Niyogi, *J. High Energy Phys.* **06** (2014) 012; N. Chamoun, H. K. Dreiner, F. Staub, and T. Stefaniak, *J. High Energy Phys.* **08** (2014) 142.
- [15] Z. Marshall, B. A. Ovrut, A. Purves, and S. Spinner, *Phys. Lett. B* **732**, 325 (2014); *Phys. Rev. D* **90**, 015034 (2014).
- [16] Y. Bai and J. Berger, [arXiv:1407.4466](https://arxiv.org/abs/1407.4466); M. Heikinheimo, M. Raidal, and C. Spethmann, *Eur. Phys. J. C* **74**, 3107 (2014); B. A. Dobrescu and A. Martin, [arXiv:1408.1082](https://arxiv.org/abs/1408.1082).
- [17] B. Mukhopadhyaya, S. Roy, and F. Vissani, *Phys. Lett. B* **443**, 191 (1998).
- [18] E. J. Chun and J. S. Lee, *Phys. Rev. D* **60**, 075006 (1999); S. Y. Choi, E. J. Chun, S. K. Kang, and J. S. Lee, *Phys. Rev. D* **60**, 075002 (1999).
- [19] M. Hirsch, M. A. Diaz, W. Porod, J. C. Romao, and J. W. F. Valle, *Phys. Rev. D* **62**, 113008 (2000); **65**, 119901(E) (2002).
- [20] E. J. Chun and S. C. Park, *J. High Energy Phys.* **01** (2005) 009.
- [21] CMS Collaboration, Report No. CMS-PAS-SUS-13-018.
- [22] S. Chatrchyan *et al.* (CMS Collaboration), *Phys. Rev. Lett.* **111**, 221801 (2013).
- [23] CMS Collaboration, Report No. CMS-PAS-SUS-14-011.
- [24] H. M. Lee, V. Sanz, and M. Trott, *J. High Energy Phys.* **05** (2012) 139.
- [25] V. Barger, P. Huang, M. Ishida, and W.-Y. Keung, *Phys. Lett. B* **718**, 1024 (2013).
- [26] S. Heinemeyer, W. Hollik, and G. Weiglein, *Phys. Rep.* **425**, 265 (2006).
- [27] L. J. Hall, D. Pinner, and J. T. Ruderman, *J. High Energy Phys.* **04** (2012) 131.
- [28] W. Beenakker, S. Brensing, M. Kramer, A. Kulesza, E. Laenen, and I. Niessen, *J. High Energy Phys.* **08** (2010) 098.
- [29] LHC SUSY Cross Section Working Group, <https://twiki.cern.ch/twiki/bin/view/LHCPhysics/SUSYCrossSections>.
- [30] CMS Collaboration, Report No. CMS-PAS-SUS-13-019.

- [31] J. Alwall, M. Herquet, F. Maltoni, O. Mattelaer, and T. Stelzer, *J. High Energy Phys.* **06** (2011) 128.
- [32] T. Sjostrand, S. Mrenna, and P.Z. Skands, *J. High Energy Phys.* **05** (2006) 026.
- [33] M. Cacciari, G.P. Salam, and G. Soyez, *Eur. Phys. J. C* **72**, 1896 (2012).
- [34] G. Aad *et al.* (ATLAS Collaboration), *J. High Energy Phys.* **06** (2014) 035.
- [35] G. Aad *et al.* (ATLAS Collaboration), *Phys. Rev. D* **90**, 052001 (2014).
- [36] ATLAS Collaboration, Report No. ATLAS-CONF-2013-051.